# Nonlinear optical response of Au nanorods for broadband pulse modulation in bulk visible lasers

Shuxian Wang, Yuxia Zhang, Jun Xing, Xinfeng Liu, Haohai Yu' , Alberto Di Lieto, Mauro Tonelli, Tze Chien Sum, Huaijin Zhang' , and Qihua Xiong'

# Nonlinear optical response of Au nanorods for broadband pulse modulation in bulk visible lasers

Shuxian Wang,[1,2] Yuxia Zhang,[1] Jun Xing,[2] Xinfeng Liu,[2] Haohai Yu,[1,a)] Alberto Di Lieto,[3] Mauro Tonelli,[3] Tze Chien Sum,[2] Huaijin Zhang,[1,a)] and Qihua Xiong[2,4,a)]

[1]State Key Laboratory of Crystal Materials and Institute of Crystal Materials, Shandong University, Jinan 250100, China
[2]Division of Physics and Applied Physics, School of Physical and Mathematical Sciences, Nanyang Technological University, Singapore 637371
[3]NEST Istituto Nanoscienze-CNR and Dipartimento di Fisica dell'Università di Pisa, Largo B. Pontecorvo 3, Pisa 56127, Italy
[4]NOVITAS, Nanoelectronics Centre of Excellence, School of Electrical and Electronic Engineering, Nanyang Technological University, Singapore 639798

Due to the lack of suitable optical modulators, directly generated $Pr^{3+}$- and $Dy^{3+}$-doped bulk visible lasers are limited in the continuous-wave operation; yet, pulsed visible lasers are only sparingly reported recently. It has been theoretically predicated that Au nanorods could modulate the visible light operation, based on the nonlinear optical response of surface plasmon resonance. Here, we demonstrate the saturable absorption properties of Au nanorods in the visible region and experimentally realized the pulsed visible lasers over the spectral range of orange (605 nm), red (639 nm), and deep red (721 nm) with Au nanorods as the optical modulator. We show that Au nanorods have a broad nonlinear optical response and can serve as a type of broadband, low-cost, and eco-friendly candidate for optical switchers in the visible region. Our work also advocates the promise of plasmonic nanostructures for the development of pulsed lasers and other plasmonic devices. © 2015 AIP Publishing LLC. [http://dx.doi.org/10.1063/1.4934528]

Pulsed visible lasers are attractive and play important roles in the fields of technological applications and scientific research,[1–3] such as metal processing, ultra-fast dynamic observation, complex reaction detection, and medical surgery.[4,5] With regard to the generation of pulsed visible lasers, these can be obtained either from a conversion of mature infrared lasers using the nonlinear technique[2,3] or by means of direct lasing with suitable gain media,[1,6] which has some advantages in the aspects of compact structure, large conversion efficiency, and high stability. Passive pulse modulation in direct lasing could be realized in simple and compact resonant cavities, and is dominating in the low and moderate laser regimes.[4,6] For a solid-state pulsed laser, the pump source, the laser material, and the optical modulator are the three key components.[7–11] In recent years, blue diodes and laser materials are well developed, which boost the research progress of the directly generated continuous-wave bulk visible lasers.[5] However, the shortage of suitable and mature optical modulators in the visible region constrains the development of directly generated visible pulsed lasers. Although a complexly designed semiconductor saturable absorber has modulated the pulsed red laser, the fabricated cost is relatively expensive, and the corresponding response band is limited.[5,12] Additionally, the previously wide use of dye solutions in the visible pulse modulation was mostly poisonous and unstable.[13] Therefore, visible optical switchers with a broadband response, low cost, and innocuity are desirable and under-researched.

Au nanorods (NRs), as a representative of Au nanoparticles, aroused much more research interest in optics and optoelectronics.[14,15] The kinetic mechanisms about the nonlinear processes of surface plasmon resonance in Au NRs have been the subject of increasing investigations in recent years.[16,17] The surface plasmon resonance corresponds with the absorption of photons at a broadband spectral band and is tunable by the distribution and the aspect ratio of the Au NRs. With the increase of incident light intensity, the saturable absorption characteristic of Au NRs, one kind of third-order nonlinearity, would appear.[16,18] The existence of strong and broadband saturable absorption around the two relevant plasmon peaks at moderate optical intensities makes Au NRs interesting and promising in terms of pulse modulation, beside its designability and innocuity. Recently, some theoretical calculations have proposed the application feasibility of Au NRs in the visible pulse modulation.[19,20] Nevertheless, to date, there have been no experimental reports about the pulse modulation of the Au NRs in that region. In this letter, by controlling the aspect ratio of Au NRs, the Au NRs with broadband absorption in the visible region were synthesized. The saturable absorption properties of the Au NRs were systematically investigated and analyzed in the spectral areas of orange (605 nm), red (639 nm), and deep red (721 nm), respectively, which showed that the saturable absorption of the Au NRs was dispersive. The pulsed visible lasers were also demonstrated with a single optical modulator fabricated by Au NRs at those three wavelengths.

a)Authors to whom correspondence should be addressed. Electronic addresses: haohaiyu@sdu.edu.cn; huaijinzhang@sdu.edu.cn; and Qihua@ntu.edu.sg

The as-grown Au NRs were synthesized using the modified seeded growth method developed by Ye *et al.*[21] In order to ensure that the longitudinal surface plasmon resonance (LSPR) covers the applicable visible region, oxidation was used to dispose the as-grown Au NRs.[22] 133 $\mu$l of 1.5 mol/l HCl solution was added into the 10 ml of the as-grown Au NRs solution followed by bubbling air into the mixture solution for 1 min. The mixture solution was kept at 70 °C for 24 h. 1 ml of the final Au NR products was centrifuged three times at 5000 rpm (for 7 min each time) followed by the removal of the supernatant. 500 $\mu$l of deionized water and 500 $\mu$l of 1 wt.% sodium carboxymethylcellulose (NaCMC) solution obtained by ultrasonic dissolution were mixed with the final centrifuged product of the Au NRs. And then, 60 $\mu$l of final solution was evenly dropped onto a commercial glass wafer ($22 \times 22 \times 0.17$ mm$^3$), and the film was kept at room temperature to dry for about 24 h.

The size distribution of the as-grown Au NRs was counted by a scanning electron microscope (SEM) and is shown in Fig. 1(a). The Au NRs exhibit an aspect ratio of $1.63 \pm 0.35$, which is calculated from dividing the length value in the longitudinal direction by the average diameter value. After oxidation, the aspect ratio of the Au NRs declines to $1.52 \pm 0.40$. As shown in the inset of Fig. 2, the corresponding LSPR peak is located at the wavelength of 625 nm. Compared to the condition in the growth solution, the LSPR peak of Au NRs (about 660 nm) in the Au NRs-NaCMC/Glass film has a slight redshift due to the change with respect to the dielectric constant of the environment around the Au NRs.[23] As displayed in Fig. 2, the prepared Au NR films are of a wide absorption response in the visible region ranging from 500 nm to 800 nm. This wide absorption range is attributed to the transverse surface plasmon resonance (TSPR) and LSPR of the Au NRs, and benefits the development of broadband visible saturable modulators. In addition, a dimension icon atomic force microscopy (AFM) was used to investigate the quality of the fabricated sample. As demonstrated in Fig. 1(b), the fluctuation of the sample surface is relatively small.

The surface plasmon resonance of the Au NRs at different wavelengths not only could cause different linear absorptions but could also lead to different nonlinear absorptions.[16] In order to analyze the relationship between the saturable absorption and the wavelength, the investigation of the fabricated NRs-NaCMC/glass sample at the three wavelengths (605 nm, 639 nm, and 721 nm) was carried out by a femtosecond Ti:sapphire amplifier (Coherent Legend) with a pulse duration of 120 fs and a repetition rate of 1 kHz. The
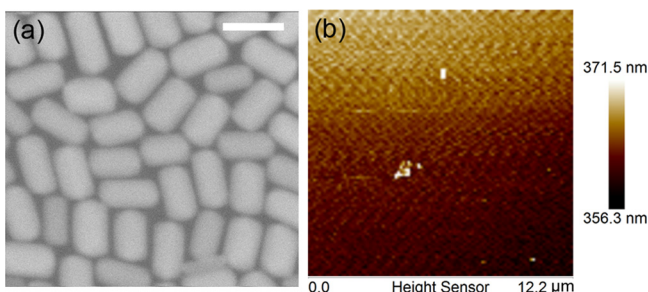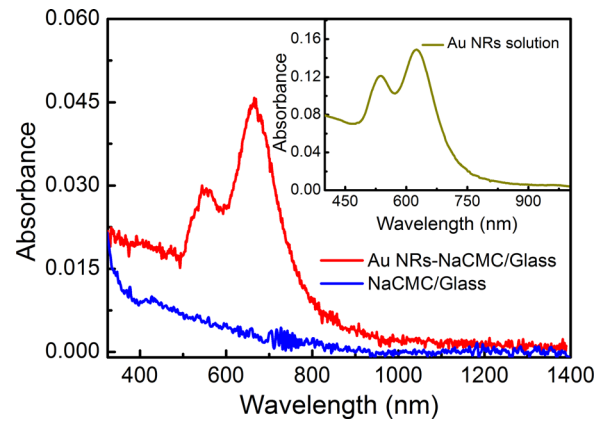


FIG. 2. Absorption spectra of the Au NRs-NaCMC/Glass film and NaCMC/Glass film. Inset: Absorption spectrum of the as-grown Au NRs solution with oxidation.

saturable absorption process could be studied by the analysis model of a two-level saturable absorber, and the power-dependent transmission formula is described as[24]

$$T = A \exp\left(\frac{-\delta T}{1 + I/I_{sat}}\right),\qquad(1)$$

where $T$ is the normalized transmittance of the sample, $A$ is the normalization constant, $\delta T$ is the absolute modulation depth of the sample, $I$ is the incident intensity, and $I_{sat}$ is the saturation intensity. Elim *et al.* reported that when the laser irradiance is above 7 GW/cm$^2$, reverse saturable absorption would become the dominant nonlinear absorption effect in Au NRs.[16] In order to avoid the reverse saturable absorption influence as far as possible, the maximum optical intensity used in the measurement was controlled below 3.5 GW/cm$^2$. In Fig. 3, the saturable absorption properties of the Au NRs sample were exhibited at the wavelengths of 605 nm, 639 nm, and 721 nm, respectively. Eq. (1) was employed to fit the surveyed data, the absolute modulation depth $\delta T$ is determined to be 7.3% at 605 nm, 10.6% at 639 nm, and 5.9% at 721 nm, and the saturation intensity $I_{sat}$ is calculated to be 49.6 MW/cm$^2$ at 605 nm, 75.0 MW/cm$^2$ at 639 nm, and 49.5 MW/cm$^2$ at 721 nm. The existence of saturable absorption at moderated pump intensities for the three wavelengths further makes the pulse modulation of the Au NRs film in the visible



FIG. 1. (a) SEM photograph of the as-grown Au NRs with a scale bar of 100 nm. (b) AFM image of the fabricated Au NRs-NaCMC/Glass film.
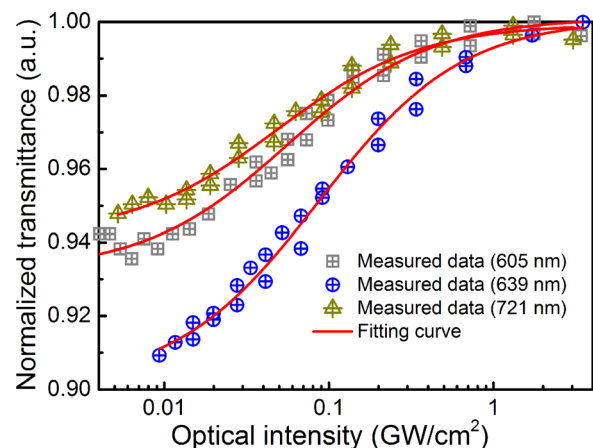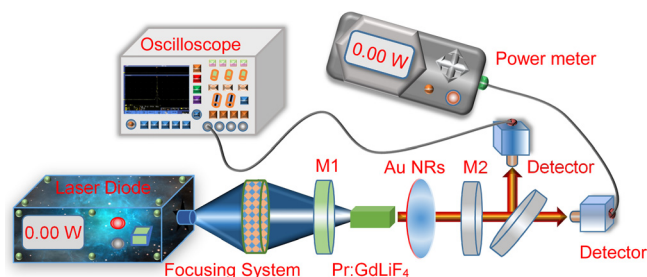


FIG. 3. Dependence of normalized transmittance on the optical intensity for the wavelengths at 605 nm, 639 nm, and 721 nm, respectively.

FIG. 4. Experimental setup of Pr:GdLiF$_4$ pulsed laser.

region possible. The larger saturation intensity at 639 nm should be associated with the large linear absorption as shown in Fig. 2, where more electrons need to be excited for attaining the saturation state. This mechanism can be verified by the comparable saturation intensity at 605 nm and 721 nm where the linear absorption is almost the same. Besides, the relatively large absolute modulation depth and the saturation intensity at 639 nm suggest that the fabricated Au NRs sample would be more promising at this wavelength.

As displayed in Fig. 4, a simple plano-concave resonant cavity was used to test the Q-switching performance of the Au NRs-NaCMC/Glass film. A laser diode with a central wavelength of 445 nm was employed as the pump source. A lens with a focus length of 25 mm was used to focus the pump light by passing through the input plane mirror, which has an antireflection (AR) coating for the pump wavelength on the side of the laser diode and a high reflective (HR)

coating for the laser wavelength (550–780 nm) on the side of the intracavity. An uncoated and polished *a*-cut Pr:GdLiF$_4$ crystal with the dimensions of $2.5 \times 2 \times 6.9 \, \text{mm}^3$ $(a \times c \times a)$ was used as the gain material because Pr$^{3+}$ ions have rich emission lines from green to deep red regions, and the low phonon energies in the fluoride host are beneficial for the generation of efficient Pr$^{3+}$-doped lasers.[6,25] In order to remove the heat generated in the laser process, the gain medium was wrapped by an indium foil and mounted in a copper block cooled by water at 7 °C. The different Q-switched lasers, including orange (605 nm), red (639 nm), and deep red (721 nm) pulse lasers, were obtained with the use of corresponding output couplers. All the output mirrors have a radius of curvature of 50 mm, and the transmittance is about 4% at 605 nm, 1.8% at 639 nm, and 1.4% at 721 nm, respectively. The optimized length of the cavity has few changes for all the Q-switched lasers and is about 45 mm. In the pulsed laser operation, the Au NRs saturable absorber is inserted into the different cavity configurations as close as possible to the output mirror to augment the pump power above the oscillated threshold; the corresponding Q-switched lasers at the respective output wavelengths would then be obtained. The output power was measured by a power meter (1916-R, Newport, Inc.), and the temporal pulse behaviors of the Q-switched lasers were recorded by a TDS3012 digital oscilloscope (100 MHz bandwidth and 1.25 GS/s sample rate, Tektronix, Inc.).

As shown in Figs. 5(a), 5(c), and 5(e), all the values of the average output power at the three different wavelengths
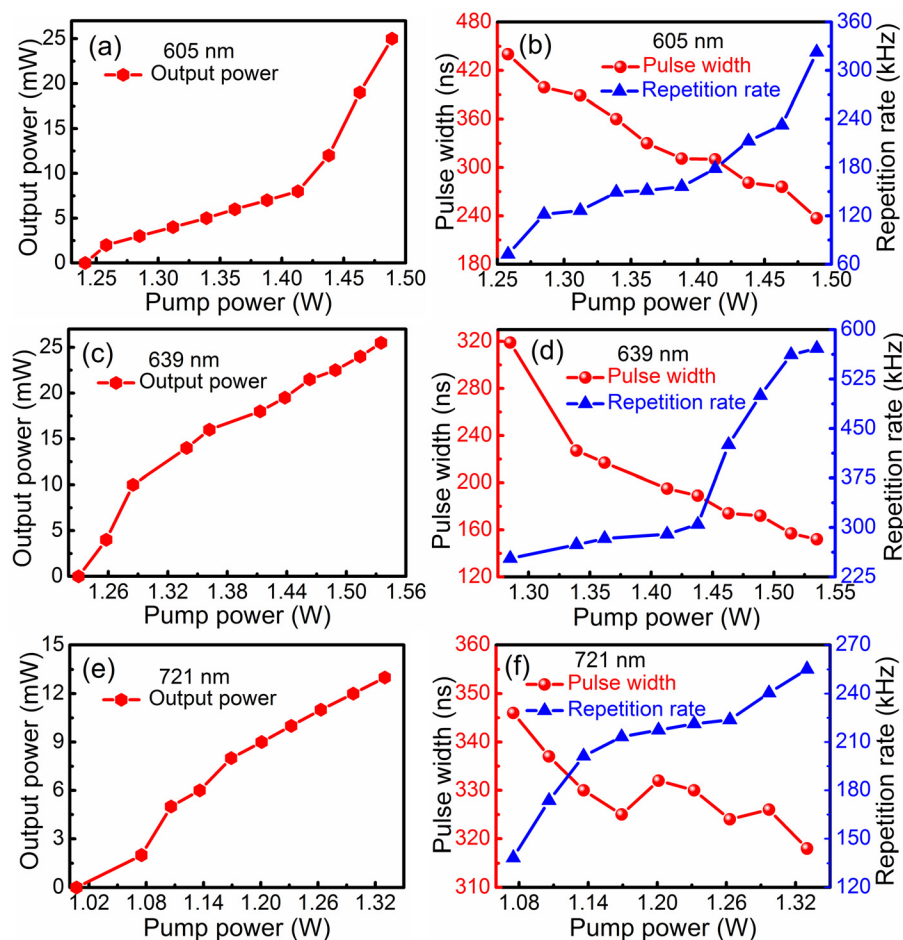


FIG. 5. Average output power versus pump power for the wavelengths at 605 nm (a), 639 nm (c), and 721 nm (e), respectively. The pulse width and pulse repetition frequency versus pump power for the wavelengths at 605 nm (b), 639 nm (d), and 721 nm (f), respectively.

increase with augmenting the pump power. The obtained maximum Q-switched output power is 25 mW, 25.5 mW, and 13 mW at the wavelengths of 605 nm, 639 nm, and 721 nm, respectively. In the laser operation, when the pump power exceeds a threshold, the Q-switched lasers at the wavelengths of 605 nm and 639 nm would be unstable. The values of the unstable threshold are 1.49 W at 605 nm and 1.33 W at 721 nm. Nevertheless, albeit the Au NRs sample in the laser cavity at 639 nm endures a larger laser intensity compared with those at 605 nm and 721 nm, the Q-switched laser performance at 639 nm still keeps stable when the laser diode almost reaches the attainable power of 1.53 W. The appearance of the unstable pulse modulation at the two wavelengths of 605 nm and 721 nm should be related to the processes of reverse saturable absorption in the Au NRs, e.g., two-photon absorption and free-carrier absorption.[16,26,27] On the basis of the discussion about the saturable absorption properties at the three wavelengths in the above-mentioned section, the saturation intensity at 639 nm is larger than that at 605 nm and 721 nm. Therefore, the unstable threshold at 639 nm should be higher than that at 605 nm and 721 nm.

As exhibited in Figs. 5(b), 5(d), and 5(f), for the different output wavelengths, the pulse repetition frequencies show an increasing tendency while the pulse widths display a decreasing tendency in the dependence on the increase of the pump power. Both the shortest pulse width and the largest pulse repetition frequency for those three wavelengths were achieved at the same moment when the respective maximum output power was obtained. The maximum repetition rate is 323 kHz, 571 kHz, and 255 kHz at the wavelengths of 605 nm, 639 nm, and 721 nm, respectively, and the minimum pulse width is 237 ns at 605 nm, 152 ns at 639 nm, and 318 ns at 721 nm. As presented in Figs. 6(a)–6(c), the single pulses at different wavelengths are equally symmetric, suggesting that the matching between the modulation depth of the Au NRs sample and the output coupling was appropriate.[28] The

corresponding pulse trains displayed in Fig. 6(d) are clean and stable, indicating the excellent Q-switching properties of the Au NRs.

The generated pulse width of the Q-switched laser could be surveyed by the theoretical calculation derived from the analysis model for semiconductor saturable absorbers[28]

$$\tau_P = \frac{3.52 T_R}{\delta T}, \tag{2}$$

where $\tau_P$ is the pulse width of the Q-switched laser, $T_R$ is the cavity round-trip time, and $\delta T$ is the modulation depth. As measured in the above section, the modulation depth of the Au NRs sample is 7.3% at 605 nm, 10.6% at 639 nm, and 5.9% at 721 nm. Besides, the cavity length has few changes for the three different Q-switched lasers, and it is about 45 mm. By use of Eq. (2), it is noteworthy that the pulse modulation of the Au NRs sample would have the smallest pulse width at 639 nm and the largest pulse width at 721 nm. The experimental minimum pulse widths at the three wavelengths coincide well with the varying tendencies between the pulse width and wavelength in the qualitative analysis. With a combination of the values of the pulse repetition rate and the average output power, the pulse energy could be calculated. The maximum pulse energy is 81.7 nJ at 605 nm, 64.0 nJ at 639 nm, and 51 nJ at 721 nm for the pump power of 1.46 W, 1.44 W, and 1.33 W, respectively. Taking advantage of the calculated pulse energies and measured pulse widths, the magnitude of peak power could be obtained, and the largest peak power is 0.33 W at 605 nm, 0.34 W at 639 nm, and 0.16 W at 721 nm for the pump powers of 1.49 W, 1.44 W, and 1.33 W, respectively. We believe that the pulsed laser performance would be further improved by optimizing the modulation depth of the Au NRs and designing suitable dielectric coatings on the laser crystal. Combined with the reported pulse modulation of the Au nanoparticles in Yb-doped fibers (1 μm) and Er-doped fibers
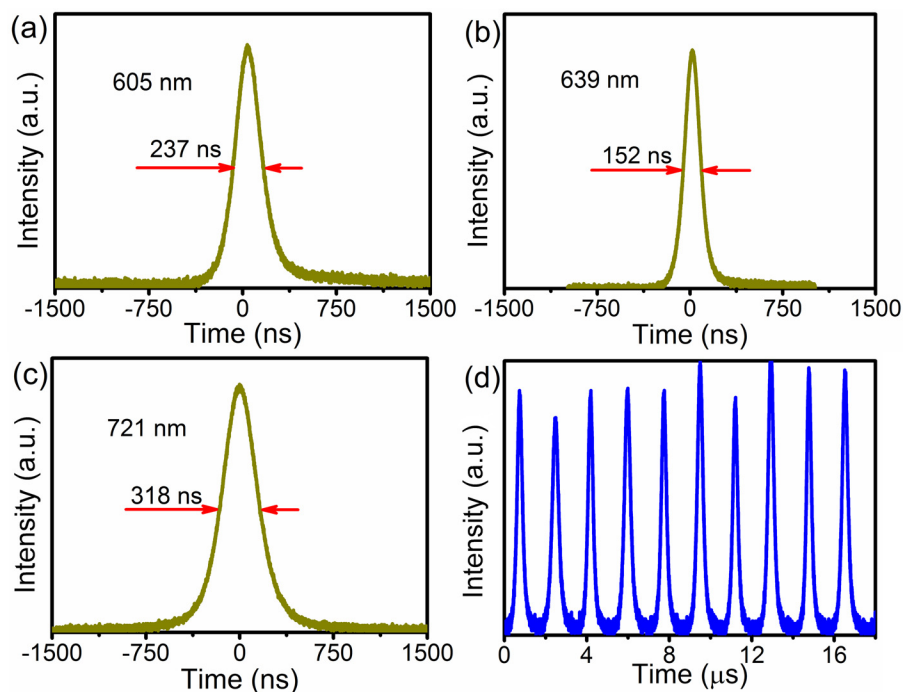


FIG. 6. Pulse profiles under the pump power of 1.49 W for 605 nm (a), 1.53 W at 639 nm (b), and 1.33 W at 721 nm (c). (d) Pulse train under the pump power of 1.53 W at 639 nm.

(1.56 $\mu$m), it is worth noting that the Au nanoparticles could be proposed as potential broadband saturable absorbers by regulating their size, shape, or aggregation.[29–32]

To sum up, the exploration of the applicable Au nanorods switchers was carried out to solve the existing problem of the lack of available optical modulators in the pulsed visible lasers. The dispersive saturable absorption properties of Au nanorods were measured and analyzed in detail at different visible wavelengths ranging from 605 nm to 721 nm. Then, using a single visible optical switcher fabricated by the Au nanorods, the corresponding orange (605 nm), red (639 nm), and deep red (721 nm) pulsed lasers were achieved. Our results indicate that Au nanorods are of potential applications in the visible pulse modulation, which will broaden the application areas of these in optoelectronics and point out a practicable development route for metal nanoparticles in the field of visible optical switching.

[1]S. Calvez, J. E. Hastie, M. Guina, O. G. Okhotnikov, and M. D. Dawson, Laser Photonics Rev. **3**, 407 (2009).
[2]D. C. Parrotta, A. J. Kemp, M. D. Dawson, and J. E. Hastie, IEEE J. Sel. Top. Quantum Electron. **19**, 1400108 (2013).
[3]P. J. Campagnola and L. M. Loew, Nat. Biotechnol. **21**, 1356 (2003).
[4]H. M. Pask, P. Dekker, R. P. Mildren, D. J. Spence, and J. A. Piper, Prog. Quantum Electron. **32**, 121 (2008).
[5]U. Keller, Nature **424**, 831 (2003).
[6]P. W. Metz, F. Reicher, F. Moglia, S. Müller, D. Marzahl, C. Kränkel, and G. Huber, Opt. Lett. **39**, 3193 (2014).
[7]Y. Shimony, Z. Burshtein, and Y. Kalisky, IEEE J. Quantum Electron. **31**, 1738 (1995).
[8]A. Ikesue and Y. L. Aung, Nat. Photonics **2**, 721 (2008).
[9]G. Boulon, Opt. Mater. **34**, 499 (2012).
[10]W. B. Cho, J. H. Yim, S. Y. Choi, S. Lee, A. Schmidt, G. Steinmeyer, U. Griebner, V. Petrov, D. I. Yeom, K. Kim, and F. Rotermund, Adv. Funct. Mater. **20**, 1937 (2010).
[11]L. A. Coldren, S. W. Corzine, and M. L. Mashanovitch, *Diode Lasers and Photonic Integrated Circuits*, 2nd ed. (Wiley, Hoboken, 2012), Chap. 2.
[12]U. Keller, K. J. Weingarten, F. X. Kartner, D. Kopf, B. Braun, I. D. Jung, R. Fluck, C. Hönninger, N. Matuschek, and J. A. Au, IEEE J. Sel. Top. Quantum Electron. **2**, 435 (1996).
[13]J. C. Diels and W. Rudolph, *Ultrashort Laser Pulse Phenomena*, 2nd ed. (Elsevier, Burlington, 2008), Chap. 3.
[14]P. C. Ray, Chem. Rev. **110**, 5332 (2010).
[15]A. Kuzyk, R. Schreiber, H. Zhang, A. O. Govorov, T. Liedl, and N. Liu, Nat. Mater. **13**, 862 (2014).
[16]H. I. Elim, J. Yang, J. Y. Lee, J. Mi, and W. Ji, Appl. Phys. Lett. **88**, 083107 (2006).
[17]G. A. Wurtz, R. Pollard, W. Hendren, G. P. Wiederrecht, D. J. Gosztola, V. A. Podolskiy, and A. V. Zayats, Nat. Nanotechnol. **6**, 107 (2011).
[18]Z. Kang, Y. Xu, L. Zhang, Z. Xia, L. Liu, D. Zhao, Y. Feng, G. Qin, and W. Qin, Appl. Phys. Lett. **103**, 041105 (2013).
[19]K. H. Kim, U. Griebner, and J. Herrmann, Opt. Express **20**, 16174 (2012).
[20]K. H. Kim, U. Griebner, and J. Herrmann, Opt. Lett. **37**, 1490 (2012).
[21]X. Ye, C. Zheng, J. Chen, Y. Gao, and C. B. Murray, Nano Lett. **13**, 765 (2013).
[22]T. Ming, L. Zhao, Z. Yang, H. Chen, L. Sun, J. Wang, and C. Yan, Nano Lett. **9**, 3896 (2009).
[23]S. K. Ghosh and T. Pal, Chem. Rev. **107**, 4797 (2007).
[24]W. D. Tan, C. Y. Su, R. J. Knize, G. Q. Xie, L. J. Li, and D. Tang, Appl. Phys. Lett. **96**, 031106 (2010).
[25]F. Cornacchia, A. D. Lieto, M. Tonelli, A. Richter, E. Heumann, and G. Huber, Opt. Express **16**, 15932 (2008).
[26]F. Hache, D. Ricard, C. Flytzanis, and U. Kreibig, Appl. Phys. A **47**, 347 (1988).
[27]M. Perner, S. Gresillon, J. März, G. V. Plessen, and J. Feldmann, Phys. Rev. Lett. **85**, 792 (2000).
[28]G. J. Spühler, R. Paschotta, R. Fluck, B. Braun, M. Moser, G. Zhang, E. Gini, and U. Keller, J. Opt. Soc. Am. B **16**, 376 (1999).
[29]T. Jiang, Y. Xu, Q. J. Tian, L. Liu, Z. Kang, R. Y. Yang, G. S. Qin, and W. P. Qin, Appl. Phys. Lett. **101**, 151122 (2012).
[30]Z. Kang, X. Y. Guo, Z. X. Jia, Y. Xu, L. Liu, D. Zhao, G. S. Qin, and W. P. Qin, Opt. Mater. Express **3**, 1986 (2013).
[31]D. F. Fan, C. B. Mou, X. K. Bai, S. F. Wang, N. Chen, and X. L. Zeng, Opt. Express **22**, 18537 (2014).
[32]Z. Kang, Q. Li, X. J. Gao, L. Zhang, Z. X. Jia, G. S. Qin, and W. P. Qin, Laser Phys. Lett. **11**, 035102 (2014).